Mon. Not. R. astr. Soc. (1978) **185**, 207–225

The spectrum of small-scale density fluctuations in the solar wind

A. C. S. Readhead, M. C. Kemp and A. Hewish

Mullard Radio Astronomy Observatory, Cavendish Laboratory, Madingley Road, Cambridge CB3 0HE

Received 1978 March 20; in original form 1977 November 9

Summary. Interplanetary scintillation observations at frequencies between 74 and 1400 MHz and solar elongations in the range 10–90° are combined to determine the form of the wavenumber spectrum of electron density fluctuations in the range $10^{-3} < k < 10^{-1}$/km (where $k = 2\pi/\lambda$). The data are best explained by a spectrum in which there is a genuine scale-length; they are not consistent with a simple power-law spectrum. This suggests that turbulence may be less important than some kind of plasma instability in generating small-scale density fluctuations. The relevance of these conclusions to the use of IPS for determining radio source structure is discussed.

1 Introduction

Interplanetary scintillation (IPS) is caused by fluctuations of electron density in the solar wind having scales between about 10 and 200 km. The determination of the spectrum of these fluctuations is not straightforward since observed parameters of the diffraction pattern require careful correction for the effects of source size and Fresnel filtering. Considerable uncertainty has therefore existed concerning the form of the spectrum.

When the first measurements from spacecraft became available it was suggested (Cronyn 1972; Jokipii 1973) that IPS observations could be explained by a simple power-law spectrum extending over scales of 10 to 10^6 km. Unfortunately this model is inadequate. Rickett (1973) showed that the wavelength dependence of IPS is incompatible with a simple power-law model, confirming the earlier conclusions of Hewish (1971) and Matheson & Little (1971). Similar conclusions have been reached by Lotova (1975). To explain the wavelength dependence of scintillation index it is necessary to adopt a spectrum which is considerably flatter than the extrapolated spacecraft spectrum at temporal frequencies below about 1 Hz. Independent evidence of such a flattening has also been obtained from spacecraft measurements (Neugebauer 1975; Unti & Russell 1976).

In spite of the failure of the simple power-law model, it is still frequently regarded as the *best* first approximation to the irregularity spectrum for IPS purposes (Coles, Rickett & Rumsey 1974; Milne 1976; Coles & Kaufman 1977) and Armstrong & Coles (1978) have

suggested that the survey by Readhead & Hewish (1974), the results of which were analysed using a Gaussian model of the spectrum, should be reinterpreted on the basis of a power-law spectrum. Since experience with the 4.5-acre telescope has demonstrated that scintillation versus solar elongation curves can now be obtained with less uncertainty than the discrepancies in the angular diameters derived from the different models, it is therefore important to determine the irregularity spectrum with greater precision.

We believe that the earlier discussions of the spectrum by Readhead (1971); Rickett (1973); Houminer (1973) and Lotova (1975) can now be considerably improved for the following reasons.

(a) There has been a considerable increase in IPS data which now extend over a wide range of radio frequency and solar elongation. In particular, temporal IPS power spectra are available and these were not seriously considered by Rickett or Lotova.

(b) Improved computational methods and a more detailed scattering-theory have removed the necessity for some simplifying assumptions made in earlier work – such as weak scattering, or a physically-thin scattering layer.

(c) More is known about the angular sizes of radio sources so that corrections for diameter blurring can be applied with greater confidence. This is especially important at low radio frequencies where 'ideal point sources' do not exist.

In this paper we derive a more accurate spectrum of the irregularities in the wavenumber range $10^{-3} < k < 10^{-1}$/km and we confine our attention to distances between 0.1 and 1.5 AU. At smaller distances there is evidence that temporal IPS spectra may be generated both by internal rearrangement and by outward convection of time-stationary irregularities, and interpretation of the observations becomes difficult.

In Section 2 we summarize the observational data and discuss their relevance in testing different aspects of the wavenumber spectrum. In Section 3 an attempt is made to find a satisfactory simple power-law model in order to highlight the inadequacies of this approach. This is followed, in Section 4, by consideration of a simple Gaussian spectrum characterized by a scale-size which varies with distance from the Sun. It is found that this model gives a very satisfactory fit to the data and provides an excellent first approximation to the irregularity spectrum. At high wavenumbers the observations indicate that the actual spectrum falls slightly more slowly than a Gaussian. The power in this range is small, however, and may be readily explained if the actual density irregularities are slightly less 'smooth' than the ideal Gaussian form (Matheson & Little 1971). In Section 5 we summarize our conclusions and compare the parameters of the best-fitting Gaussian model with other models derived previously. Our present results are in fair agreement with Readhead's (1971) work for distances exceeding 0.5 AU but indicate a larger scale-size at shorter distances. This leads to revised values of angular sizes in the survey by Readhead & Hewish (1974) and these are described. The geometry of the problem is shown in Fig. 1, and some useful definitions and results in scintillation theory are collected for convenience in an Appendix.

2 The observational data

2.1 PROBLEMS OF INTERPRETATION

Several difficulties arise in determining the spectrum of the density variations from IPS data. Components larger than the size of the first Fresnel zone (about 700 km at 81.5 MHz at 0.5 AU) are removed by a diffraction limit known as the Fresnel filter; this becomes more important at higher radio frequencies and at large solar elongations. Components of small

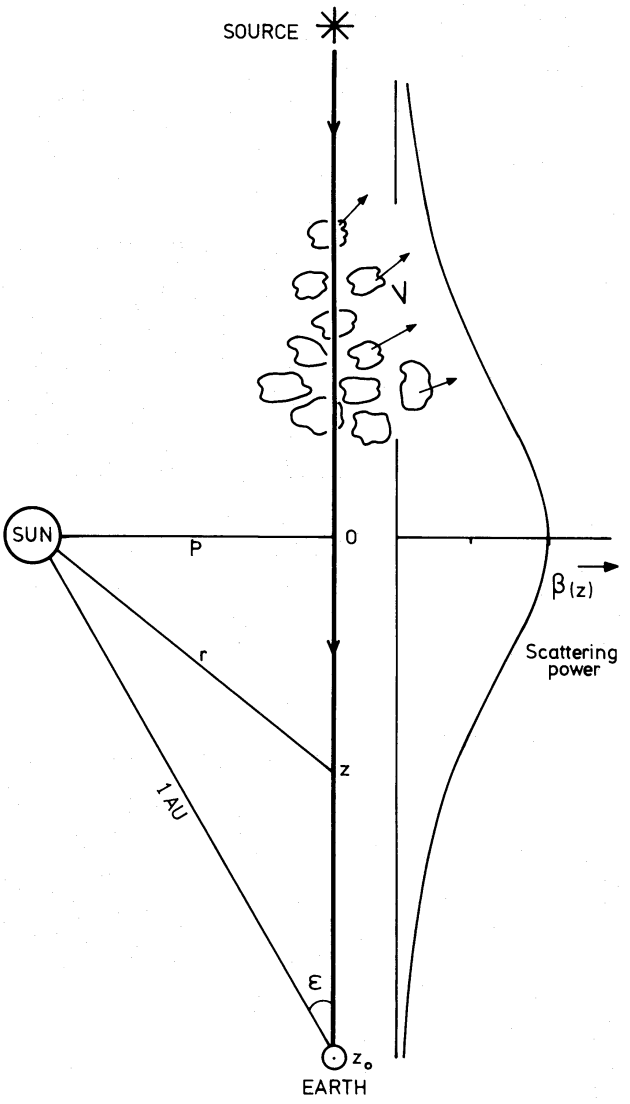

Figure 1. Geometry of the interplanetary medium.

scale, on the other hand, may be removed by blurring arising from the finite angular size of a radio source or a finite receiver bandwidth; these are more important at lower radio frequencies and at small elongations. In our attempt to find a satisfactory spectrum we adopt some simple models and adjust their parameters, making careful allowance for the above effects, to give the following data. (Consult the Appendix for a definition of terms.)

(1) The variation of scintillation index m with elongation ϵ and radio wavelength λ.

(2) The dependence of the first moment ν_1 (or τ) on ϵ and λ. Values of the second moment ν_2 are often quoted but we regard this as a less accurate parameter than ν_1 since it gives greater weight to components of small scale which are weaker and subject to greater errors due to the smaller signal/noise ratio. We therefore use the first moment in preference to the second moment.

(3) The shape of $P(v)$.

(1), (2) and (3) are employed at elongations large enough for the weak-scattering approximation to be valid. At small elongations the $m(\epsilon)$ curve has a maximum and then

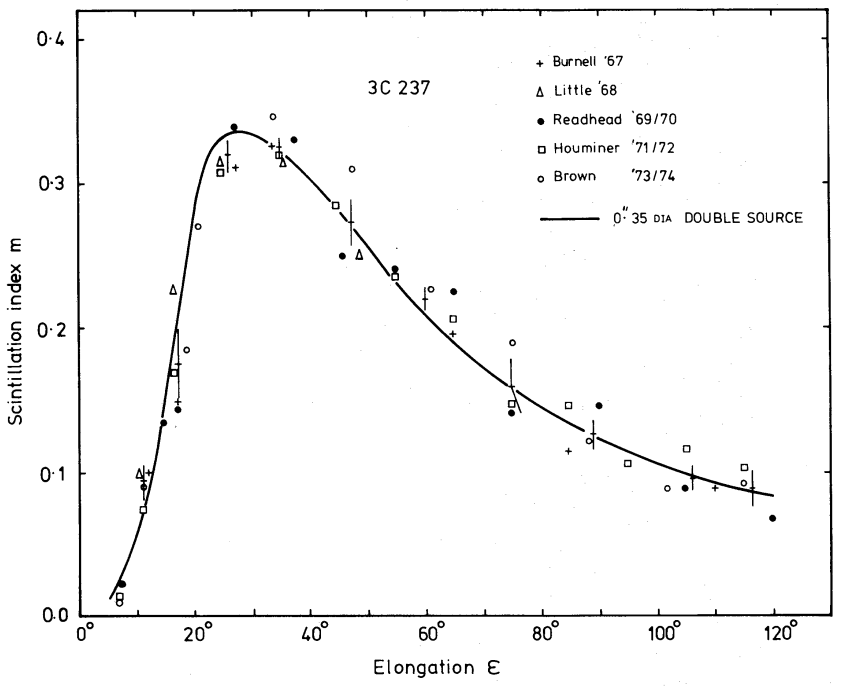

Figure 2. Scintillation index versus elongation for the source 3C 237, observed at Cambridge over eight years. Also shown is a theoretical curve for a symmetrical double source, each component of which has a diameter of 0.35 arcsec.

falls rapidly with decreasing elongation. This is associated with the onset of strong scattering and in this region we also use:

(4) The limiting slope of $m(\epsilon)$ at small elongations.

Observations made a different times may be subject to errors due to changes in the solar plasma, perhaps correlated with the solar cycle. However, no evidence for long-term variations has been found for $\epsilon > 10^\circ$ (Houminer 1973). Solar-wind streams of different velocity, which persist for one or two rotations, cause day to day variations of m which can be as large as a factor of 2 or 3 (Houminer & Hewish 1972). These errors can be reduced to

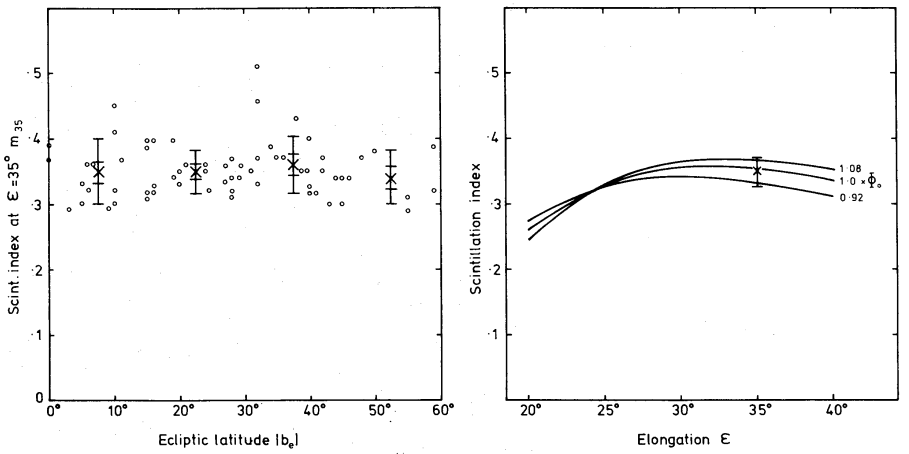

Figure 3. Variation of scattering power with ecliptic latitude. (a) Scintillation index at 35° plotted against ecliptic latitude of the point of maximum scattering along the line of sight. Observed values of m were averaged in 15° bins and the bars denote standard deviation. (b) Variation of $m(\epsilon)$ with scattering power Φ_0, showing the limits placed on any ecliptic latitude variation.

about ±10 per cent by averaging over 10 day. The overall reproducibility of IPS measurements can be gauged from Fig. 2 in which the $m(\epsilon)$ curves for 3C 237 are shown for eight years during 1967–74. The data for 1971/72 were by Houminer who measured relative, rather than absolute, values of m. His data were calibrated by comparison of 12 sources (excluding 3C 237) for 1971 January–June, with Readhead's observations for the same sources during 1970 July–December.

It is assumed that the density variations are not dependent upon heliocentric latitude. Since there is now evidence for a systematic latitude dependence of solar wind velocity (Coles & Rickett 1976) some variation might be expected. No dependence of m with latitude has, however, been found. This is shown in Fig. 3(a) where $m(35°)$ has been plotted for 70 sources for which the line of sight passes nearest to the Sun at a variety of latitudes. The sources were chosen to have angular diameters in the range 0.3 to 0.5 arcsec and were classified as A or B in the survey by Readhead & Hewish (1974). The limits that the data place on variations with latitude can be seen in Fig. 3(b), in which are shown curves for different scattering powers computed on the Gaussian model with a diameter of 0.4 arcsec.

2.2 THE DATA

The following observations have been used in our analysis.

A 1410 MHz

Bourgois (1976, private communication); $m(\epsilon)$ for elongations $\epsilon < 30°$, for the sources PKS 1148–00 and 1504–16.7. These sources have the flat radio spectra typical of sources with angular sizes of a few milliarcsec, and may be regarded for our purpose as ideal point sources. Also we have measurements of v_1 for the 13 sources 3C 273, 3C 279, CTA 21, PKS 0019+00, 0056−00, 0802+21, 0400+25, 0428+20, 0851+20, 1038+06, 1148−00, 1504−16.7, 2128−12.

B 408 MHz

Milne (1976); v_1 and m in the range $5° < \epsilon < 25°$, for the sources PKS 0019−00, 0056−00, 0316+16, 1148−00, 2203−18. These were Milne's least-resolved sources; they have flat spectra and the point-source assumption is again made.

C 151.5 MHz

Duffett-Smith (1976); $m(\epsilon)$ curves for $\epsilon > 20°$ for the sources CTA 21, 3C 48, 119, 147, 237, 287. The angular diameters derived from the $m(\epsilon)$ curves are given in Duffett-Smith & Readhead (1976).

D 81.5 MHz

Little (private communication); τ for $\epsilon > 35°$ for the sources 3C 119, 138, 186, 216, 237 and 238; Dennison (1967) for 3C 48. Houminer (1973); $P(v)$ for the sources 3C 48, 237, 241 and 287. Burnell, Readhead, Houminer, Brown (in preparation); $m(\epsilon)$ for $\epsilon > 35°$ for the sources 3C 48, 119, 147, 237. These curves are unpublished but angular diameters and other parameters based upon them have been given by Burnell (1968), Houminer (1973) and Readhead & Hewish (1974).

E 74 MHz

Coles *et al.* (1974); Armstrong & Coles (1972); $m(\epsilon)$, pattern scale and $P(v)$ for 3C 144 at elongations of $10^\circ < \epsilon < 90^\circ$.

3 The power-law model

In this section we attempt to find a power-law spectrum of the irregularities which is consistent with all the observations. It will be assumed that the variations of electron density have a three-dimensional spectrum of the form $P_N(k) = A(r)k^{-\alpha}$, where $k = (k_x^2 + k_y^2 + k_z^2)^{1/2}$ is the wavenumber given by 2π/(spatial wavelength), and $A(r)$ describes how the strength of the variations depends upon radial distance, r, from the Sun. It is assumed that the spectrum is both isotropic and time stationary.

The value of α inferred from spacecraft measurements of the proton flux is $\alpha \sim 3.3$–3.6 (Unti & Russell 1976). Since the evidence for a power-law spectrum of the electron density variations was originally based on spacecraft data (Cronyn 1972), it might seem that this value should be taken, but IPS data suggest a lower value.

Values for the power-law index derived from observations D and E are as follows:

$\alpha \sim 2.6$ for $\epsilon > 30^\circ$ (one-third of data) (Coles *et al.*),
$\alpha \sim 3.0$ for $\epsilon > 30^\circ, k > 0.01$/km
$\alpha \sim 2.4$ for $\epsilon > 30^\circ, k < 0.01$/km } (two-thirds of data),
$\alpha \sim 2.4$ for $\epsilon > 30^\circ, k > 0.01$/km (Houminer).

Houminer concluded that a simple power-law could not be fitted for $k < 0.01$/km; he also made allowance for source size which reduces α. It should be noted that Coles *et al.* could not fit a simple power law to the bulk of their data. In attempting to derive the best-fitting power law, we initially put $\alpha = 2.5$ and investigate the wavelength dependence of the sctintillation index and first moment v_1.

3.1 THE WAVELENGTH DEPENDENCE OF m

For a physically-thin layer of irregularities at a distance z, Matheson & Little (1971) have shown that

$$m \propto \lambda^{(\alpha+2)/4} z^{(\alpha-2)/4} \quad \text{for } 2 < \alpha < 6.$$

The thin-layer approximation leads to negligible errors for $\epsilon \lesssim 30^\circ$, and the value $\alpha = 2.5$ gives a predicted wavelength dependence $m \propto \lambda^{1.12}$ for the power-law model in this elongation range.

Directly measured values of the product mf (data A for $\epsilon < 30^\circ$) are shown in Fig. 4. Many observations have been combined to produce the points shown in the figure. At 1410 MHz each point represents about 30 independent measurements. These are assumed to refer to point sources and hence required no correction for resolution. Values of the product (data C and D for $\epsilon > 30^\circ$) for the least-resolved sources lie along the dashed line shown in Fig. 4. Before using these data it is necessary to make a correction for the source size at 151 and 81.5 MHz which amounts to an increase in m of roughly 30 per cent. A comparison of the computations of Readhead (1971) and Marians (1975) shows that, for source diameters of 0.2–0.6 arcsec, the magnitude of the *correction* is the same (to within 10 per cent) whether a power-law or Gaussian irregularity spectrum is assumed. Since we have made detailed computations for the Gaussian model (see theory in the Appendix) it is convenient to use them here and the corrected value of m will then be within about 5 per cent of the

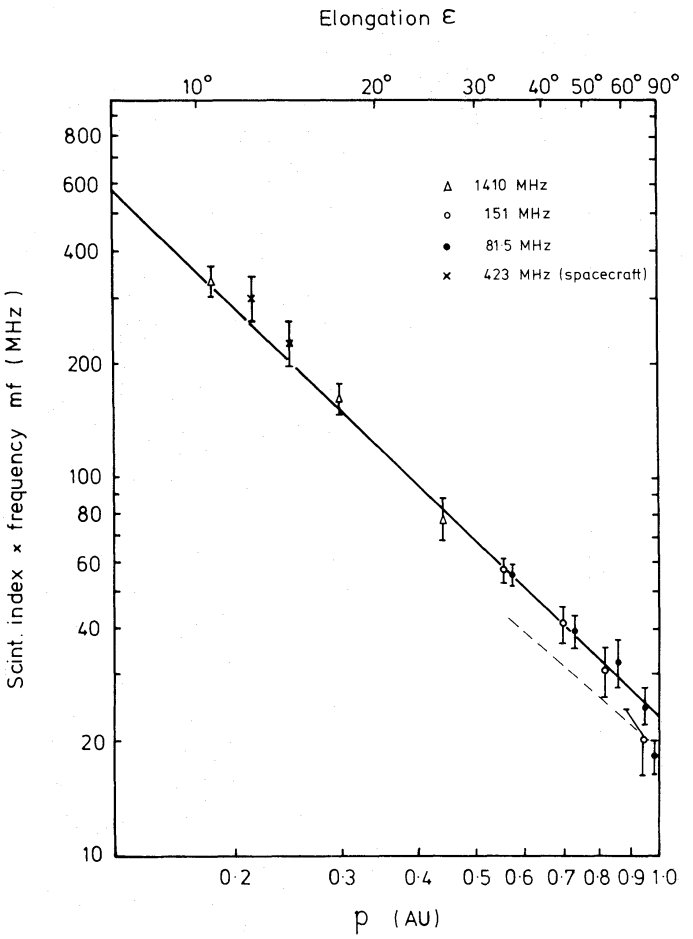

Figure 4. Scintillation index × frequency (*mf*) plotted against elongation corrected for source size effects at 151 and 81.5 MHz. The best-fitting line, drawn solid, has a slope of -1.5. The dashed line was drawn through the observed values of m (points not shown) *before* correcting for source size.

value computed for a power-law spectrum. The source diameters were derived using Readhead's (1971) method and differed slightly at 151 and 81.5 MHz. The corrections at each frequency were made *independently* and the points in Fig. 4 show corrected *mf* values. The resulting agreement between corrected scintillation indices at these two frequencies is a measure of the reliability of the method. In the range $0.2 < p < 0.8$ the points are a good fit to the straight line $mf = 23(p/\mathrm{AU})^{-1.5}$ MHz, from which we derive $m \propto f^{-1}$. The uncertainty of this frequency dependence can be tested by making separate least-squares fits in the ranges $\epsilon < 30^\circ$ and $\epsilon > 30^\circ$ and noting the discrepancy between the two lines at $\epsilon = 30^\circ$. Such an analysis shows that the frequency dependence is given by

$$m \propto f^{-(1.0 \pm 0.05)},$$

and this can be explained on the power-law model only if $\alpha < 2.5$. If, as seems very unlikely, resolution effects are important in data A and B, the value of α derived by the above method will be an overestimate, thus strengthening the upper limit for α derived here.

The values of m used in Fig. 4 were obtained by calibrated measurements of the radio flux density of the scintillating signal from several sources. As has been discussed above, the 81.5- and 151-MHz results have been corrected for partial resolution by the medium, but the correction is not strongly model-dependent, and we could equally well have used corrections derived from the power-law model. Armstrong & Coles (1978) have adopted an

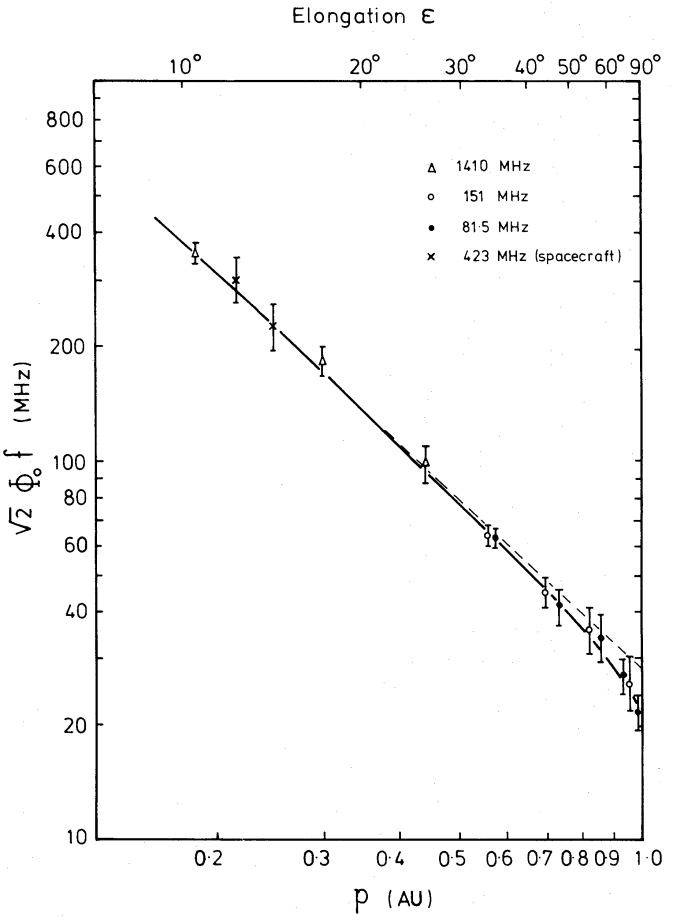

Figure 5. The points in Fig. 4 corrected for Fresnel filtering using the Gaussian model discussed in the text. The solid line is that predicted for a scattering power of $\beta(r) = 2.73 \times 10^{-3} \lambda^2 r^{-4}$ rad²/AU. The dashed line, of slope -1.5, is the asymptote close to the Sun.

alternative method of deriving the point-source scintillation index curve, which is based on the power-law model and which is strongly model-dependent. Their values at 74 MHz lie roughly 30 per cent above the line in Fig. 4. If this value is taken as an upper limit, since we believe it to be an overestimate, the relation $m \propto f^{-1.15}$ is obtained.

Combining the results of these independent methods shows that the observed wavelength dependence of m can only be satisfied if $\alpha \lesssim 2.5$. On the Gaussian model described in Section 4, $m \propto f^{-1}$ (approximately) and the values of Φ_0 derived from the points in Fig. 4 should scale exactly as f^{-1}, as shown in Fig. 5.

An independent check of our mf relation has recently come from spacecraft scintillation studies at 423 MHz (Chang 1976). The number of observations made so far is small but the source-size problem is completely removed owing to the point-source nature of the transmitter. As may be seen in Fig. 4, the measurements are in good agreement with calibrated IPS values. No correction has been made for the fact that the transmitter was embedded in the scattering medium, since the magnitude of the required correction is < 5 per cent.

3.2 WAVELENGTH DEPENDENCE OF ν_1

The first moment of the observed temporal IPS spectrum may be calculated as follows for the power-law model. Small wavenumbers will be cut off by the Fresnel filter; we designate

this cutoff frequency ν_F. There will also be some higher frequency, ν_u, which is the limit at which the spectrum can be accurately measured due to the system noise level.

Assuming a thin-screen model, the slope of the temporal spectrum in the range $\nu_F < \nu < \nu_u$ will be $(\alpha - 1)$ (Cronyn 1972). The first moment is then given approximately by

$$\nu_1 = \nu_F \cdot \frac{\frac{1}{2} + [(\nu_F/\nu_u)^{\alpha-3} - 1]/(3-\alpha)}{1 + [(\nu_F/\nu_u)^{\alpha-2} - 1]/(2-\alpha)}.$$

The thin-screen assumption is good for $\epsilon < 30$. If $\nu_u \gg \nu_F$ the relation simplifies to:

$\nu_1 \propto \nu_F$ for $\alpha > 3$,

$\nu_1 \propto \nu_F^{\alpha-2}\nu_u^{3-\alpha}$ for $2 < \alpha < 3$.

Now, since ν_F is the cutoff due to the Fresnel filter, $\nu_F \propto \lambda^{-1/2}$.

This analysis may be applied to observations close to the Sun at 1410 and 408 MHz (data A and B). The first moments derived from these observations are shown in Fig. 6. At $\epsilon = 15°$ we have

ν_1(1410 MHz) = 0.8 ± 0.05 Hz,

ν_1(408 MHz) = 0.7 ± 0.1 Hz.

The difference between the two values of ν_1 is hardly significant, showing immediately that $\alpha < 3$. Putting $\alpha > 3$ leads to $\nu_1 \propto \lambda^{-0.5}$ which is a significantly stronger dependence on wavelength than is observed. An upper limit to the observed wavelength dependence is $\nu_1 \propto \lambda^{-0.25}$. This corresponds to $\alpha = 2.5$ if we set ν_u equal at each frequency. We therefore conclude that $\alpha < 2.5$ for the power-law index.

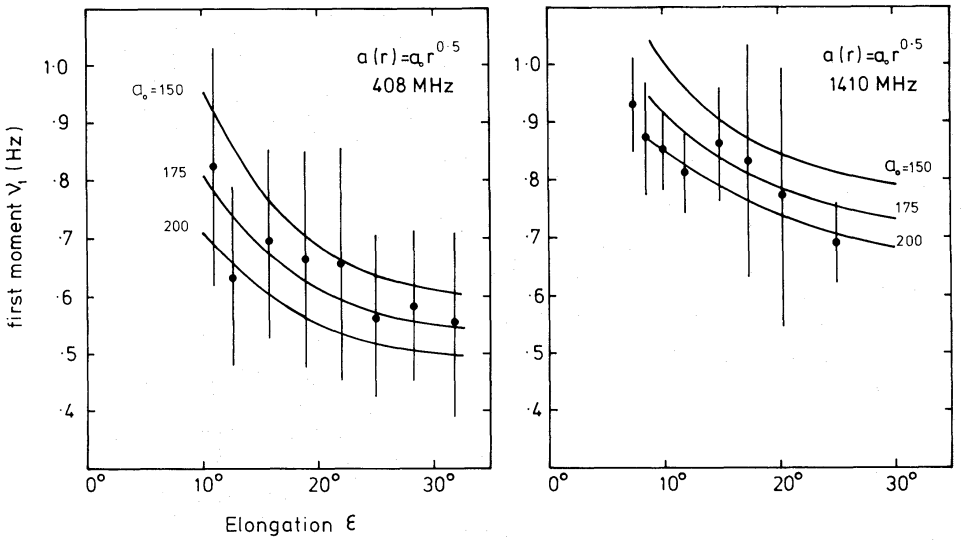

Figure 6. Observations of the first moment of the temporal spectrum compared with theoretical curves for Gaussian models described in the text. (a) 408-Mhz data (Milne), (b) 1410-MHz data (Bourgois).

3.3 THE LIMITING SLOPE OF $m(p)$ FOR SMALL p

Observations of a radio source of finite angular size always show a rapid decline in scintillation index at small elongations due to the onset of strong scattering. Rumsey (1975) shows (his equation 39 *et seq.*), for the case of a thin screen with strong scattering, that

$m_{ext} \propto U^{-1/(\alpha-2)}$ for $\alpha > 2$,

where U is the intensity randomization. U is the square of the point-source scintillation index that would be obtained from the Born approximation. Now, from Fig. 4, for the weak-scattering case where m_{pt} is indeed given by the Born approximation, we see that

$$m_{pt}^2 = U \propto p^{-3}.$$

Hence we expect for the limiting slope of $m_{ext}(p)$

$$m_{ext}(p) \propto p^{3/(\alpha-2)}.$$

This result is strictly true only in the strong-scattering limit. However, theoretical curves computed by Marians (1975) for the case $\alpha = 3$ show that, for all sources of diameter $2\theta_0 \gtrsim 0.5$ arcsec, the $m_{ext}(p)$ curve deviates insignificantly from its asymptote for elongations $\epsilon < 15^\circ$ and by less than 10 per cent for $\epsilon < 20^\circ$, using their value for U.

In Table 1 the slopes $\delta(\log m)/\delta(\log p)$ in the range $10^\circ < \epsilon < 20^\circ$ are shown for four sources which have been observed by Brown at 81.5 MHz (data D). These observations give a mean slope $m(p) = p^{(1.9 \pm 0.15)}$ from which we derive $\alpha = 3.6 \pm 0.2$ for the simple power-law model. Note that the adoption of a model with $\alpha = 2.5$ leads to $m(p) \propto p^6$!

Table 1. Observed values of the slope of $m(p)$ at small elongations.

Source	$\delta(\log m)/\delta(\log p)$
3C 67	1.8 ± 0.1
3C 144	2.1 ± 0.2
3C 237	2.0 ± 0.15
3C 241	1.7 ± 0.15

3.4 OBSERVATIONS OF SCATTERING ANGLE

We note here that observations of θ_s, the scattering angle of waves from a point source in the strong-scattering regime, imply a value of power-law index similar to that in the previous section. Observations of the wavelength dependence of θ_s (Hewish 1958) show that $\theta_s \propto \lambda^2$. It may be shown using the same theory as in the previous section (Rumsey) that a power-law index $\alpha = 4$ is needed to satisfy this dependence. We note, however, that these observations were made close to the Sun ($p < 0.1$), and may not be strictly comparable with the results of the previous sections.

3.5 DISCUSSION

The value $\alpha < 2.5$ obtained by the two different methods in Sections 3.1 and 3.2 is clearly inconsistent with the value $\alpha = 3.6$ predicted in Section 3.3, and also the values $\alpha = 3.0$–3.6 obtained from observations of the tails of temporal spectra. The value $\alpha = 3.6$ is also the value inferred from spacecraft spectra and the assumption of Kolmogorov turbulence. It must therefore be concluded that a simple power-law model cannot account for all the IPS data. A more complex model, perhaps with a break in the spectrum or with a power-law index changing with elongation, might possibly give a better fit. This, however, is tantamount to assuming that genuine scale lengths exist in the solar plasma.

If this is so, we believe that a simpler model, as described in the next section, represents a more satisfactory approach.

4 The Gaussian model

If the spectrum of the irregularities is characterized by some genuine scale-length it is convenient to try fitting a model of the form

$$P_N(k) = \frac{a^2}{4\pi}\beta(r)\exp(-k^2a^2/4),$$

where we make the same assumptions about isotropy and spherical symmetry as in Section 3. As a further simplification the parameters $\beta(r)$ and $a(r)$ are assumed to vary with solar distance such that $\beta(r) = A_0 r^{-b}$ and $a(r) = a_0 r^{\delta}$. We now outline our method of determining these parameters.

The first step is to refer to high-frequency measurements in the region $0.1 < p < 0.5$ where the scattering is weak and the measurements are least affected by source size. Crude estimates of the scale-size, ignoring the effect of Fresnel filtering, can be obtained from measurements of ν_1 and τ. These show that a is not large enough for Fresnel filtering to reduce the scintillation index by more than about 20 per cent. It is thus a good approximation to put

$$m^2 \propto \Phi_0^2 = \int_{-\infty}^{z_0} \beta(r)\,dz$$

(see Appendix). The observations that have already been discussed in Section 3 show that $m \propto p^{-1.5}$ for $p < 0.5$ and, since the upper limit of integration in the expression for m can be taken as infinite when p is small, we obtain $\beta(r) \propto r^{-4}$. Having found the radial dependence of $\beta(r)$ we can now use weak-scattering theory to integrate along the line of sight, assuming different values of a_0 and δ, until the computed estimates of ν_1 and τ agree with observed values. This leads to an accurate value of $a(r)$. The irregularity spectrum $P_N(k)$ is then fully determined in the range $r < 0.5$ AU.

At greater distances from the Sun we must use observations at lower frequencies, where corrections for source size can reach 30–40 per cent. Our procedure here is to assume that the form of $\beta(r)$ can be extended to $r > 0.5$ AU. Accurately computed values of ν_1 and τ are then compared with observation to determine the scale size $a(r)$ in this region. Having determined the scale size $a(r)$ and the form of the scattering power $\beta = A_0 r^{-4}$, we can finally allow for Fresnel filtering and source size to determine the magnitude of A_0.

The quantitative application of these methods is now described.

4.1 THE SCALE-LENGTH $a(r)$

The limitations imposed by the weak-scattering condition necessitated the use of observations at 1410 and 408 MHz in the range $0.2 < r < 0.5$ AU (data A and B), and at 74 and 81.5 MHz (data D and E) in the range $0.7 < r < 1.0$ AU. The fit of $\nu_1(\epsilon)$ for the high-frequency observations is shown for three models in Fig. 6. The best fit to both data A and B was found to be $a(r) = (175 \pm 20) r^{(0.5 \pm 0.1)}$ km.

In using data D and E it was first necessary to reduce the 74-MHz data to the same form as that at 81.5 MHz. The published values of data E were converted using the relation

$$\tau = \left(\frac{\text{observed scale length}}{\text{observed velocity}}\right)\frac{4\sqrt{2}}{5}.$$

The numerical factor of $\sqrt{2}$ converts the $e^{-1/2}$ to e^{-1} width assuming a Gaussian acf. The remaining factor allows for the fact that the measured cross-correlation functions were typically 25 per cent wider than the acf (Rickett 1973).

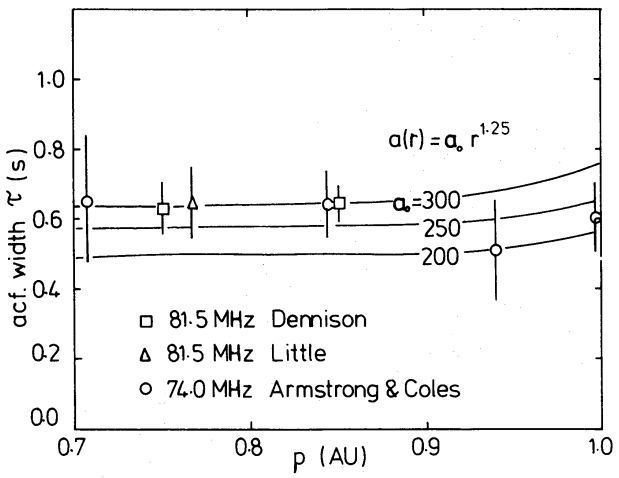

Figure 7. Observed values of the width to $1/e$ of the temporal autocorrelation function compared with theoretical curves for a 0.4-arcsec diameter source.

The data were averaged into 10° bins and compared with theoretical models in the same way as the observations for $r < 0.5$. We assumed a source diameter of 0.4 arcsec, i.e. the mean diameter of the observed sources calculated on the Gaussian model. The result is insensitive to the exact value chosen. For models with $a(r)$ varying as r^{δ} ($\delta < 1.5$), the curves $\tau(p)$ are very flat and, given the scatter in the data, it is impossible to distinguish between them. Values of $\delta > 1.5$ can, however, be ruled out by the observed lack of variation in $\tau(p)$. All the models which fit require a scale of about 250 km at 1 AU and, by continuity of the scale size with that derived for $r < 0.5$ AU, we can rule out models with $\delta < 1.0$. Thus we choose (see Fig. 7)

$$a(r) = (250 \pm 30) r^{(1.25 \pm 0.3)} \text{km} \quad \text{for } 0.7 < r < 1.0.$$

A model, consistent with all the data over the whole range of r, is obtained by combining the two expressions for $a(r)$ above. Thus we find

$$a = 175\, r^{0.5} \text{km} \ (0.1 < r < 0.6 \text{ AU})$$
$$= 250\, r^{1.25} \text{km} \ (0.6 < r < 1 \text{ AU}).$$

An independent check of this model can be made at small elongations from the limiting slope of $m(p)$ observed under conditions of strong scattering at low frequencies. It can be shown by using the same assumptions as in Section 3.3 that, if $a(r) \propto r^{\delta}$, and $m(p) \propto \Phi_0 \propto r^{-\gamma}$ for high frequencies where the weak-scattering approximation holds, we have a limiting slope $m(p) \propto p^{\delta+\gamma}$.

The observations described in Section 3.3 give $m(p) \propto p^{(1.9 \pm 0.15)}$, and putting $\gamma = 1.5$ (as shown in Section 3.1) we derive $\delta = 0.4 \pm 0.15$, which is consistent with $\delta = 0.5$ given by the model. Further refinement of the model will require more accurate values of ν_1.

It is interesting to compare the model with previous estimates of scale size obtained by different observers as shown in Fig. 8. Satisfactory agreement is generally obtained, but it is clear that Readhead's (1971) model gave scales too small at some elongations. Rao, Bhandari & Ananthakrishnan (1974) concluded that the scale did not increase significantly for $r > 0.3$ AU, and that it decreased rapidly for $r < 0.3$ AU; this behaviour is not consistent with our model, although the discrepancy is small over the limited range of r considered by Rao *et al.*

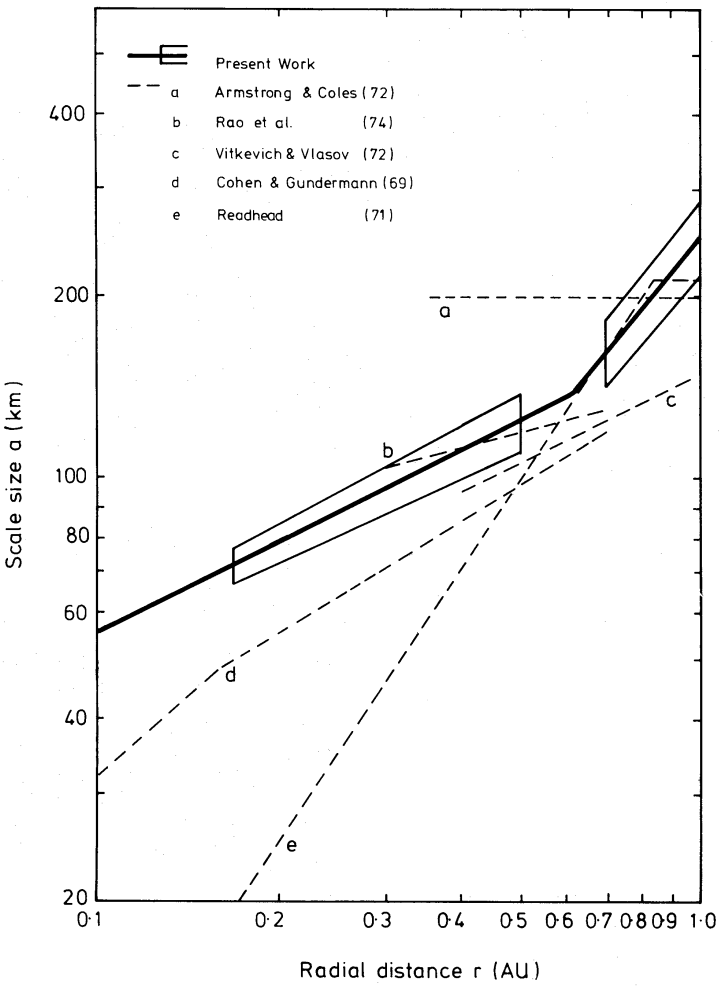

Figure 8. The variation of scale size, $a(r)$, with solar distance, showing the uncertainty in the determination. Also shown are other estimates of the scale size adjusted, where necessary, for different definitions of scale size and the value of Φ_0 used.

4.2 THE DETERMINATION OF $\beta(r)$

The radial dependence of $\beta(r) = A_0 r^{-4}$ has already been found as discussed at the beginning of this section. We now determine A_0 by making the final correction for Fresnel filtering and bandwidth, and then using the relation

$$\Phi_0^2 f^2 = \int_{-\infty}^{z_0} A_0 r^{-4}\, dz.$$

Values of $\sqrt{2}\Phi_0 f$ are plotted in Fig. 5; they differ only slightly from the points in Fig. 4, but the difference is significant. Note that the points show a significant departure from the straight line by a factor $1/\sqrt{2}$ at $p = 1$, due to the observer being immersed in the scattering medium. The best-fitting value of A_0 is found to be $A_0 = (2.73 \pm 0.15) \times 10^{-3}$, and hence $\beta(r) = 2.73 \times 10^{-3} (r/\text{AU})^{-4} (\lambda/\text{m})^2 \text{ rad}^2/\text{AU}$. The uncertainty in radial dependence is $\beta \propto r^{-(4.0 \pm 0.1)}$. In terms of the fluctuations in electron density we have (see Appendix)

$$\Delta N_e(\text{RMS}) = \begin{cases} 0.072\, r^{-2.6}\ \text{cm}^{-3} & \text{for } r > 0.6\ \text{AU} \\ 0.080\, r^{-2.3}\ \text{cm}^{-3} & \text{for } r < 0.6\ \text{AU}. \end{cases}$$

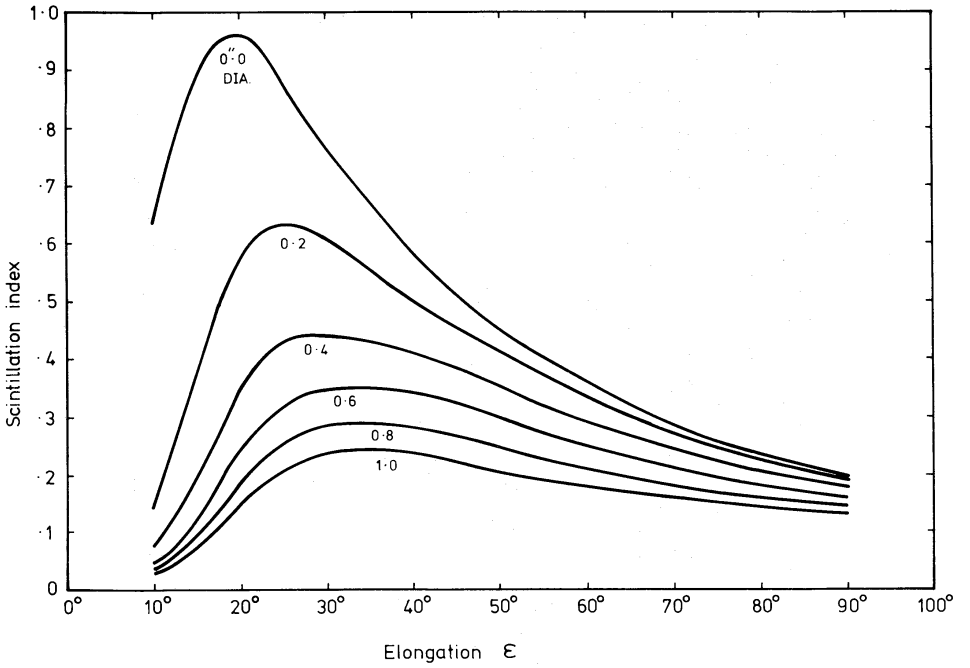

Figure 9. Scintillation index versus elongation as a function of source diameter at 81.5 MHz (Δf = 1 MHz) for the model described in the text, derived by methods described in Kemp (in preparation).

The accuracy to which the Gaussian model reproduces $m(\epsilon)$ curves over a wide range of elongation is illustrated in Fig. 2 where the best-fitting curve is compared with observations of 3C 237 at 81.5 MHz. A more exact treatment of the strong-scattering region was used in the computation. In this treatment Kemp (in preparation) calculates the scintillation index of extended sources seen through an extended medium of arbitrary scattering profile, under the assumption (which is good at 81.5 MHz) that Fresnel filtering effects are unimportant in regions where the scattering is strong. The fit is extremely good over the range $10° < \epsilon < 120°$ and with data of this quality the angular size of 3C 237 is given to an accuracy of ± 0.05 arcsec. A family of theoretical $m(\epsilon)$ curves for different source sizes is shown in Fig. 9.

Our analysis of the Gaussian model has therefore shown that the parameters can be chosen to fit the IPS data very well. None of the serious inconsistencies arise that were found for the power-law model. One feature that deserves further attention is the 'tail' of the power spectrum at large wavenumbers where the observations (see Section 3) suggest that the spectrum falls slightly more slowly than a Gaussian for $k > 3 \times 10^{-2}\,\mathrm{km}^{-1}$. The spectrum contains little power in this range, however, and in view of the observational uncertainties it seems premature to attempt further refinements until data of high signal/noise ratio at large wavenumbers are available.

5 Discussion

The main conclusion of the analyses carried out in this paper is that a simple Gaussian model of the irregularity spectrum in the range $5 \times 10^{-3} < k < 3 \times 10^{-2}\,\mathrm{km}^{-1}$ can explain a broad variety of IPS observations, whereas a simple power-law model exhibits serious inconsistencies. The arguments leading to this conclusion have been somewhat involved and the observational tests are summarized for convenience in Table 2.

Table 2. A comparison of the predictions of Gaussian and power-law models of the irregularity spectrum.

TEST	IRREGULARITY SPECTRUM		OBSERVED	FIT	
	GAUSSIAN $\exp\left[-\frac{k^2 a^2(r)}{4}\right]$	POWER LAW $k^{-\alpha}$		POWER LAW	GAUSSIAN
Scintillation index versus wavelength (point source) $m(\lambda)$	$m \propto \lambda$	$m \propto \lambda^{\left(\frac{\alpha}{4}+\frac{1}{2}\right)}$ $2 < \alpha < 6$	$m \propto \lambda^{1\cdot0 \pm \cdot05}$	$\alpha \leqslant 2$	✓
Width of temporal spectrum $\nu_t(\lambda)$	$\nu_t(\lambda) \approx a(r)$ (weak dependence on λ)	$\nu_t(\lambda) \propto \lambda^{-1/2}$ $\alpha > 3$ $\propto \lambda^{\frac{1-\alpha}{2}}$ $2 < \alpha < 3$	$\nu_t(\lambda) \propto \lambda^{<\cdot2}$	$\alpha < 2{\cdot}5$	✓
Scint. index at small elongations (strong scatt., extended source) $M_{ext}(\rho)$	$M_{ext} \propto \rho^2$	$M_{ext} \propto \rho^{\frac{3}{\alpha-2}}$	$M_{ext} \propto \rho^{1\cdot9 \pm \cdot2}$	$\alpha = 3{\cdot}6$	✓
Scattering angle versus wavelength (strong scatt.) $\theta_s(\lambda)$	$\theta_s \propto \lambda^2$	$\theta_s \propto \lambda^{\frac{\alpha}{\alpha-2}}$	$\theta_s \propto \lambda^2$	$\alpha = 4$	✓

Our revised model, described in Section 4.2, differs in two aspects from an earlier model by Readhead (1971). First, the strength of the density fluctuations is now believed to be 40 per cent greater than before, so that an ideal point source would exhibit a correspondingly larger scintillation index in the weak scattering regime. The effect of this revision is to decrease the values of R by about 40 per cent for most sources in the survey by Readhead & Hewish (1974). Second, the scale size is now known to be slightly larger at smaller elongations. The combined effect of both revisions is to reduce the quoted source diameters (in arcsec) as follows: $0.2 \rightarrow 0.15$, $0.3 \rightarrow 0.2$, $0.4 \rightarrow 0.3$, $0.6 \rightarrow 0.45$, $0.8 \rightarrow 0.6$ and $1.0 \rightarrow 0.75$. The effect of the new model on the distribution of source sizes (Hewish, Readhead & Duffett-Smith 1974) is to provide a small systematic shift in both the values of θ obtained and the resolution limit; the conclusions are thus unaltered.

Our revised model predicts values of m which are some 30 per cent lower than those of Armstrong & Coles (1978) for an ideal point source at 74 MHz. Armstrong & Coles did not attempt to derive m directly from an absolute measurement of the scintillating flux density, but used the theoretical shape of $m(\epsilon)$, assuming a simple power-law model with $\alpha = 3$. It is likely that the disagreement with our model arises from the adoption of a simple power-law irregularity spectrum which, as we have shown, is not consistent with some of the observations.

In discussion of IPS at 327 MHz, Rao *et al.* (1974) mention difficulties in accounting for the turnover of $m(\epsilon)$ at $p \sim 0.2$ AU. The predictions of our model are in good agreement with their observations (e.g. 3C 2, 3C 138, PKS 0115 − 01) if the sources have angular diameters of about 0.1–0.2 arcsec. We therefore believe that some of the angular sizes derived by Rao *et al.* using the second moment of the temporal IPS spectrum may be substantially too small.

It is interesting to compare our model of the irregularity spectrum with spacecraft measurements of the proton flux. The comparison with data by Neugebauer (1975) is shown

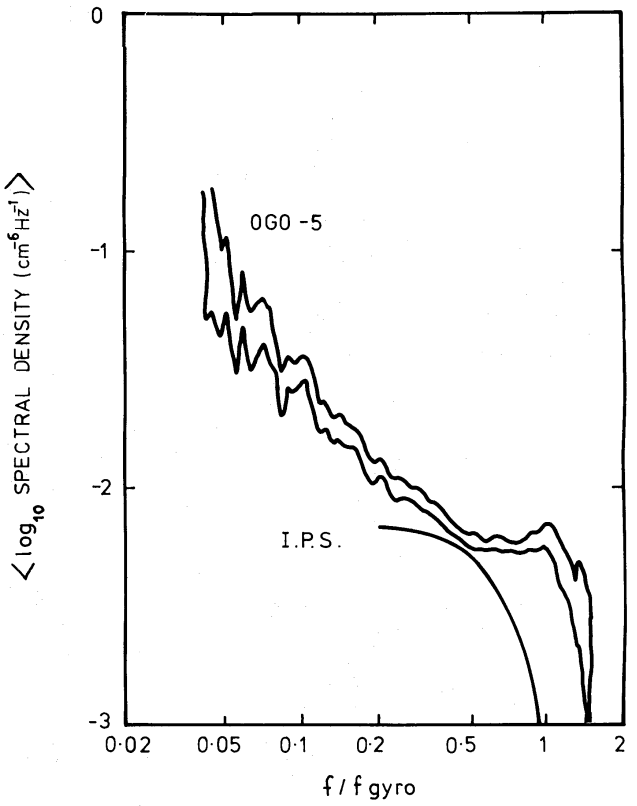

Figure 10. The temporal spectrum of electron density fluctuations observed by a space probe. Upper curves show the 90 per cent confidence interval of the *OGO-5* spectra (Neugebauer 1975), and the lower curve is the corresponding spectrum at 1 AU predicted by the present work. The frequency axis is scaled by the temporal frequency corresponding to the convection of irregularities with a scale size of the proton gyroradius.

in Fig. 10 and indicates that the IPS data give somewhat weaker fluctuations of electron density. We believe that random perturbations of the solar wind velocity, such as might arise from turbulence, could account for this difference. Density fluctuations are not measured directly by spacecraft; they are inferred from fluctuations of the particle flux. Since the magnitude of the IPS density variations is so small (~ 1 per cent of the mean density, Little 1971) it follows that a 1 per cent modulation of velocity would be sufficient to cause a serious overestimate of the inferred density fluctuations.

Acknowledgments

We thank G. Bourgois, A. G. F. Brown and L. T. Little for providing data prior to publication, and the referee for helpful comments. ACSR is indebted to the Royal Society for a fellowship supported by the Weir Foundation, MCK gratefully acknowledges the support of an SRC studentship.

References

Armstrong, J. W. & Coles, W. A., 1972. *J. geophys. Res.*, **77**, 4602.
Armstrong, J. W. & Coles, W. A., 1978. *Astrophys. J.*, **220**, 346.
Budden, K. G. & Uscinski, B. J., 1970. *Proc. R. Soc. Lond. A.*, **316**, 315.
Budden, K. G. & Uscinski, B. J., 1971. *Proc. R. Soc. Lond. A.*, **321**, 15.

Budden, K. G. & Uscinski, B. J., 1972. *Proc. R. Soc. Lond. A.*, **330**, 65.
Burnell, S. J., 1968. *PhD thesis,* University of Cambridge.
Chang, H., 1976. *Stanford University Technical Report No. 3552–1.*
Cohen, M. H. & Gundermann, E. J., 1969. *Astrophys. J.*, **155**, 645.
Coles, W. A. & Kaufman, J. J., 1977. *Mon. Not. R. astr. Soc.*, **181**, 57P.
Coles, W. A. & Rickett, B. J., 1976. *J. geophys. Res.*, **81**, 4797.
Coles, W. A., Rickett, B. J. & Rumsey, V. H., 1974. *Solar wind three,* pp. 351–367, ed. Russell, C. T.
Cronyn, W. M., 1972. *Astrophys. J.*, **171**, 4101.
Dennison, P. A., 1967. *PhD thesis,* University of Cambridge.
Duffett-Smith, P. J., 1976. *PhD thesis,* University of Cambridge.
Duffett-Smith, P. J. & Readhead, A. C. S., 1976. *Mon. Not. R. astr. Soc.*, **174**, 7.
Hewish, A., 1958. *Mon. Not. R. astr. Soc.*, **118**, 534.
Hewish, A., 1971. *Astrophys. J.*, **163**, 645.
Hewish, A., Readhead, A. C. S. & Duffett-Smith, P. J., 1974. *Nature,* **252**, 657.
Houminer, Z., 1973. *Planet. Space Sci.*, **21**, 1367.
Houminer, Z. & Hewish, A., 1972. *Planet. Space Sci.*, **20**, 1703.
Jokipii, J. R., 1973. *A. Rev. Astr. Astrophys.*, **11**, 1.
Little, L. T., 1971. *Astr. Astrophys.*, **10**, 301.
Lotova, N. A., 1975. *Sov. Phys. Uspekhi.*, **18**, 292.
Marians, M., 1975. *Radio Sci.*, **10**, 115.
Matheson, D. N. & Little, L. T., 1971. *Planet. Space Sci.*, **19**, 1615.
Milne, R. G., 1976. *PhD thesis,* University of Sydney.
Neugebauer, M., 1975. *J. geophys. Res.*, **80**, 998.
Rao, A. P., Bhandari, S. M. & Ananthakrishnan, S., 1974. *Aust. J. Phys.*, **27**, 105.
Readhead, A. C. S., 1971. *Mon. Not. R. astr. Soc.*, **155**, 185.
Readhead, A. C. S. & Hewish, A., 1974. *Mem. R. astr. Soc.*, **78**, 1.
Rickett, B. J., 1973. *J. geophys. Res.*, **78**, 1543.
Rumsey, V. H., 1975. *Radio Sci.*, **10**, 107.
Salpeter, E. E., 1967. *Astrophys. J.*, **147**, 433.
Unti, T. & Russell, C. T., 1976. *J. geophys. Res.*, **81**, 469.
Vitkevich, V. V. & Vlasov, V. I., 1972. *Sov. Astr.*, **16**, 480.

Appendix

Here we present a summary of terms and relations used in the paper. The treatment is principally for a medium with a Gaussian spectrum, but the basic definitions (equations (1) to (10)) also apply to a power-law spectrum of irregularities. References to individual results are not given and the reader is referred to the following papers for more detail: Budden & Uscinski (1970, 1971, 1972); Readhead (1971); Salpeter (1967).

The geometry is shown in Fig. 1. The medium is assumed to be spherically symmetric and the irregularities are convected radially outwards with velocity V. We consider radio waves of unit intensity, frequency f, wavelength λ, propagating from a source at $-\infty$ in the $+z$ direction.

The drifting diffraction pattern in the observing plane $z = z_0$ is characterized by the 2-D spatial spectrum of intensity $M(k_x, k_y)$ where $k = (k_x^2 + k_y^2)^{1/2}$ is the wavenumber. From this we define:

Scintillation Index, m

$$m^2 = \iint M(k_x, k_y)\, dk_x\, dk_y, \tag{A1}$$

Temporal Spectrum, $P(\nu)$

$$P(\nu) = \frac{4\pi}{V_T} \int M\left(k_x = \frac{2\pi\nu}{V_T}, k_y\right) dk_y \quad \text{for } \nu \geqslant 0, \tag{A2}$$

V_T being the transverse component of the wind velocity V. The moments of this spectrum ν_n are given by

$$\nu_n = \int_0^\infty \nu^n P(\nu)\, d\nu \Big/ \int_0^\infty P(\nu)\, d\nu. \tag{A3}$$

We also use the temporal autocorrelation function of intensity, which is the Fourier Transform of $P(\nu)$ and its width τ (to $1/e$).

We now show how $M(k_x, k_y)$ is related to the statistical properties of the medium.

The medium is defined by the (3-D) spatial spectrum of electron density fluctuations $\Phi_N(k_x, k_y, k_z)$ in the interplanetary plasma, the total mean square fluctuation being given by the integral of Φ_N. The spectrum of phase fluctuations imposed by a thin layer of thickness Δz on incident waves of wavelength λ is

$$P_N(k_x, k_y) = 2\pi r_e^2 \lambda^2 \Phi_N(k_x, k_y, k_z = 0)\, \Delta z, \tag{A4}$$

where r_e is the classical electron radius. The mean square phase deviation β imposed on the wave is termed the scattering power

$$\beta(r) = \iint P_N(k_x, k_y)\, dk_x\, dk_y. \tag{A5}$$

For irregularities uncorrelated between successive layers the total mean square phase deviation Φ_0^2 is given by

$$\Phi_0^2 = \int_{-\infty}^{z_0} \beta(r)\, dz. \tag{A6}$$

The problem of relating $M(k_x, k_y)$ to $\Phi_N(k_x, k_y, k_z)$ depends on the value of Φ_0^2. For $\Phi_0^2 \ll 1$ the situation is relatively simple. For $\Phi_0^2 \gtrsim 1$ the full problem is as yet unsolved analytically, although solutions can be found for special cases.

Here we restrict ourselves to the case $\Phi_0^2 \ll 1$ for which it can be shown that M is related to the properties of the medium and source through

$$M(k_x, k_y) = \int_{-\infty}^{z_0} P_N(k_x, k_y, r) F_r(k_x, k_y, \lambda z_1)\, \mathbf{V}^2(k_x, k_y, \theta_0, z_1)\, dz, \tag{A7}$$

where $z_1 = z - z_0$ is the distance from the layer to the observer and F_r is the Fresnel filtering factor

$$F_r(k_x, k_y, \lambda z_1) = 4 \sin^2(k^2 \lambda z_1 / 4\pi). \tag{A8}$$

$\mathbf{V}^2$ is the square of the source visibility function which is related to the brightness distribution $B(\theta)$. We set

$$B(\theta) = (1/\pi\theta_0^2) \exp(-\theta^2/\theta_0^2), \tag{A9}$$

whence

$$\mathbf{V}^2(k, \theta_0, z_1) = \exp(-k^2 \theta_0^2 z_0^2/2). \tag{A10}$$

If we take a medium with autocorrelation function $\exp(-r^2/a^2)$, then

$$P_N(k, r) = \frac{a^2(r)}{4\pi} \beta(r) \exp[-k^2 a^2(r)/4]. \tag{A11}$$

Writing

$$U = \frac{\lambda z_1}{2\pi}, \quad W = \frac{a^2 + 2z_1^2\theta_1^2}{4}, \quad S^2 = W^2 + U^2,$$

we have from equations (A7 to A11)

$$M(k) = \int_{-\infty}^{z_0} \beta(r)\,(a^2/\pi)\exp(-Wk^2)\sin^2(Uk^2/2)\,dz. \tag{A12}$$

From equation (A1) we can integrate to find the scintillation index

$$m^2 = 2\int_{-\infty}^{z_0} \beta(r)\,\frac{U^2}{W(W^2+U^2)}\,(a^2/4)\,dz, \tag{A13}$$

and from equation (A2) for the temporal spectrum

$$P(\nu) = \frac{4\pi}{V_T}\int_{-\infty}^{z_0} \frac{a^2}{2(2\pi)^{1/2}}\,\beta(r)\exp(-Wk^2)\,[\ ]\,dz \tag{A14}$$

where $[\ ] = (2/W)^{1/2} - \{(S+W)^{1/2}\cos(Uk^2) - (S-W)^{1/2}\sin(Uk^2)\}/S$ and $2\pi\nu/V_T = k$.

Substituting (A14) into (A3) and performing the integration we get an analytic expression for the first moment ν_1

$$\nu_1 = (1/m^2)\int_{-\infty}^{z_0} \beta(r)[a^2 V_T/(2\pi)^{3/2}]\,[(1/2^{1/2}W^{3/2}) - \{(S+W)^{1/2}W - (S-W)^{1/2}U\}/2S^3]\,dz. \tag{A15}$$

We can include the effect of finite observing bandwidth for the case $\Phi_0 \ll 1$ by introducing another multiplicative term in equation (A7) to represent bandwidth filtering. For a resonance bandpass of form

$$I(f) = \frac{\Delta f}{\Delta f^2 + (f - f_0)^2}, \tag{A16}$$

the effect on equations (A13) and (A14) is simply to replace W^2 by $W^2 + Ub$, where $b = \Delta f/f_0$.